SOCIETY FOR EXPERIMENTAL BIOLOGY

Journal of Experimental Botany, Vol. 72, No. 7 pp. 2419–2433, 2021
doi:10.1093/jxb/eraa587 Advance Access Publication 18 December 2020

RESEARCH PAPER

Interclonal variation, coordination, and trade-offs between hydraulic conductance and gas exchange in *Pinus radiata*: consequences on plant growth and wood density

Juan Rodríguez-Gamir[1,2,*,†], Jianming Xue[2], Dean F. Meason[3], Michael Clearwater[4], Peter W. Clinton[2] and Jean-Christophe Domec[5,6]

[1] Producción Vegetal en zonas tropicales y subtropicales, Instituto Canario de Investigaciones Agrarias (ICIA), Ctra de El boquerón s/n, 38270 San Cristóbal de La Laguna, Tenerife, Canary Islands, Spain
[2] Forest Systems, Scion, PO Box 29237, Christchurch, 8440, New Zealand
[3] Forest Systems, Scion, Private Bag 3020, Rotorua, 3046, New Zealand
[4] Environmental Research Institute, University of Waikato, Private Bag 3105, Hamilton, New Zealand
[5] Bordeaux Sciences Agro, UMR INRA ISPA 1391, Gradignan, France
[6] Nicholas School of the Environment, Duke University, Durham, NC, USA

* Correspondence: jrodriguez@icia.es
† Present address: Instituto Canario de Investigaciones Agrarias (ICIA), Ctra. de El Boquerón s/n, 38270 San Cristóbal de la Laguna, Tenerife, Spain.

Received 26 May 2020; Editorial decision 2 December 2020; Accepted 17 December 2020

Editor: Yoel Forterre, CNRS Aix-Marseille University, France

Abstract

Stem growth reflects genetic and phenotypic differences within a tree species. The plant hydraulic system regulates the carbon economy, and therefore variations in growth and wood density. A whole-organism perspective, by partitioning the hydraulic system, is crucial for understanding the physical and physiological processes that coordinately mediate plant growth. The aim of this study was to determine whether the relationships and trade-offs between (i) hydraulic traits and their relative contribution to the whole-plant hydraulic system, (ii) plant water transport, (iii) CO_2 assimilation, (iv) plant growth, and (v) wood density are revealed at the interclonal level within a variable population of 10 *Pinus radiata* (D. Don) clones for these characters. We demonstrated a strong coordination between several plant organs regarding their hydraulic efficiency. Hydraulic efficiency, gas exchange, and plant growth were intimately linked. Small reductions in stem wood density were related to a large increase in sapwood hydraulic efficiency, and thus to plant growth. However, stem growth rate was negatively related to wood density. We discuss insights explaining the relationships and trade-offs of the plant traits examined in this study. These insights provide a better understanding of the existing coordination, likely to be dependent on genetics, between the biophysical structure of wood, plant growth, hydraulic partitioning, and physiological plant functions in *P. radiata*.

Keywords: Carbon allocation, hydraulic architecture, hydraulic partitioning, photosynthesis, *Pinus radiata*, plant growth, wood density.

Abbreviations: A, net CO_2 assimilation; D, stem density;Dgr, giameter growth rate; E, transpiration rate; g_s, stomatal conductance; K_{plant}, whole-plant hydraulic con ductance;$K_{plant\text{-}l}$, leaf-specific whole-plant hydraulic conductance; K_{root}, root hydraulic conductance;$K_{root\text{-}r}$, root-specific root hydraulic conductance; K_{shoot}, shoot hydraulic conductance; $K_{shoot\text{-}l}$, leaf-specific shoot hydraulic conductance; k_{stem}, stem conductivity; $k_{stem\text{-}sw}$, sapwood-specific stem conductivity; Ngr, needle growth rate;Pgr, plant growth rate; Rgr, root growth rate; Sgr, stem growth rate; T_p, whole-plant transpiration.

Introduction

Greater wood production would be economically advantageous for commercial forestry operations around the world and beneficial for the global environment as forests indisputably result in increased carbon storage and help mitigate CO_2 emissions to the atmosphere (Knauf *et al.*, 2015). Stem growth is a major component of carbon allocation in woody plants and reflects genetic and phenotypic differences within a tree species (Lambers *et al.*, 2008). The photosynthesis and respiration rates on a leaf area basis, together with the total leaf area, co-determine the relative growth rate of the plant (increase in plant mass/unit plant mass/time) (Evans, 1972; Poorter *et al.*, 2012). The carbon sequestered through photosynthesis is partially (30–50%) used for a net production of biomass and partially (50–70%) for plant metabolic processes (Marthews *et al.*, 2012). The plant hydraulic system is closely related to the carbon economy (Sack *et al.*, 2003; Zhu *et al.*, 2013). Several studies have highlighted the coordination between plant water transport capacity and leaf-level gas exchange or photosynthetic capacity (Sperry *et al.*, 1993; Brodribb and Feild, 2000; Brodribb *et al.*, 2002; Santiago *et al.*, 2004; McCulloh *et al.*, 2019). It is therefore assumed that a high plant hydraulic efficiency (i.e. high leaf-specific conductance and sapwood area-specific conductivity) is an essential prerequisite for high tree productivity (Hubbard *et al.*, 2001; Tyree, 2003; Domec *et al.*, 2015).

The plant hydraulic system has been described as an analogue of an electrical circuit (van den Honert, 1948) where the hydraulic conductance of each plant organ (root, shoot, stem, branches, or leaves) contributes in different amounts to the total conductance of the hydraulic pathway (Johnson *et al.*, 2016). Partitioning of hydraulic conductance supports the concept that hydraulic design is coordinated across the plant and plays a crucial role in plant adaptation to the environment and stress conditions (Meinzer, 2002; Drake *et al.*, 2015; McCulloh *et al.*, 2019). This coordinated design of the plant hydraulic network to match metabolic demand is a hallmark for plant selection in different species (West *et al.*, 1999; Price *et al.*, 2007; Savage *et al.*, 2010). Although the hydraulic coordination between plant organs was hypothesized >30 years ago (Zimmermann, 1983; Tyree and Ewers, 1991), relatively little is known about the relationship between hydraulics of different plant organs (e.g. root and shoots) within the plant hydraulic continuum (Alder *et al.*, 1996; Sperry and Ikeda, 1997; Martínez-Vilalta *et al.*, 2002; Pratt *et al.*, 2010), and particularly with reference to their relative effect on gas exchange and plant growth (Domec *et al.*, 2009; Black *et al.*, 2011; Attia *et al.*, 2015).

Wood density is particularly important for both wood quality and understanding tree physiological acclimation to changing growing conditions. It is an excellent predictor of mechanical properties of wood because both the modulus of rupture and the modulus of elasticity are positively correlated with wood density (Niklas, 1992; Downes *et al.*, 2002; Cown *et al.*, 2004; Lasserre *et al.*, 2009). In commercial forests, wood production has significantly increased through intensive silvicultural management and tree breeding programmes (Kimberley *et al.*, 2015; Moore and Clinton, 2015) that have been frequently focused on increased growth rates to the detriment of wood quality (Wu *et al.*, 2007; Bouffier *et al.*, 2009; Li *et al.*, 2012). Wood density reflects the final balance of carbon investment during wood formation, namely the conversion of soluble carbon (carbohydrates) into structural carbon (cellulose, hemicelluloses, and lignin) and the proportion of wall thickness and lumen area in a wood cell (Chave *et al.*, 2006; Rathgeber *et al.*, 2006; Downes *et al.*, 2009; Dalla-Salda *et al.*, 2011). Wood density correlates well with hydraulic traits in simple tracheid-based species (Hacke *et al.*, 2001; Lachenbruch and McCulloh, 2014). In *Pinus* sp., stem water transport efficiency is strongly negatively correlated with increasing wood density (Domec and Gartner, 2003; Creese *et al.*, 2011; Rosner *et al.*, 2019). Conifer conduits are only composed of medium-size tracheids, whereas in general angiosperm wood presents large vessels and small tracheids. The difference in wood structure and wood density between angiosperms and conifers allows comparison of how water transport and hydraulic safety respond to water stress (Hacke *et al.*, 2001; Carnicer *et al.*, 2013).

Pinus radiata (D. Don) is the most widely planted conifer for commercial forestry in the world (Mead, 2013). Significant gains in *P. radiata* productivity have been achieved due largely to genetic improvement and the deployment of selected clones (Burdon *et al.*, 2008; Baltunis and Brawner, 2010). Research is underway to identify specific hydraulic thresholds of this species for their inclusion in existing process-based productivity models (Stone *et al.*, 2012). A whole-organism perspective for the understanding of tree hydraulics may be particularly informative in disentangling the processes and feedbacks that mediate *P. radiata* growth and biomass production. Additionally, plant traits such as hydraulic conductance, carbon uptake and allocation, wood characteristics, and growth are strongly interrelated (Brodribb and Feild, 2000; Hölttä *et al.*, 2009; Sperry, 2011; Sala *et al.*, 2012). However, they may not be able to be optimized simultaneously owing to underlying biophysical constraints: the result is trade-offs between these traits that may apply within the species. Thus, the study of the coordination of plant functional traits within a tree species can be justified for two reasons. First, multiple relationships between functional traits between species have been described in a number of studies (e.g. hydraulic conductance with gas exchange; Zhu *et al.*, 2013); however, it is unknown if relationships and trade-offs between plant traits persist within the same species (Albert *et al.*, 2010; Laforest-Lapointe *et al.*, 2014). Second, the functional trait variability within a species influences its ability to respond to changes in climate, site, or other environmental factors (Nicotra *et al.*, 2010; Laforest-Lapointe *et al.*, 2014; Gallart *et al.*, 2019).

The aim of this study was to assess the extent of genetic interclonal variation for hydraulics, gas exchange, growth, and wood density characteristics within a population of commercially available *P. radiata* clones for the New Zealand forest

industry and determine whether the common trade-offs between these traits could be established at the interclonal level. Given that the studied genotypes were exposed to the same environmental conditions, the relationships and trade-offs detected at this scale were expected to reflect true functional relationships. The specific objectives of the present study were therefore to evaluate: (i) the coordination between the hydraulic traits within plants (root, shoot, and stem); (ii) the effect of plant hydraulics on plant water uptake; and (iii) the trade-offs between wood density and plant hydraulic parameters and the consequences on plant water use, gas exchange, and growth.

Materials and methods

Plant material, growth conditions, and experimental design

We used ten 1-year-old *P. radiata* genotypes (hereafter clones C15, C24, C28, C30, C31, C35, C37, C44, C48, and C50) supplied by Forest Genetics Ltd (FG) (Rotorua, New Zealand). These genotypes were selected from clonally tested progenies developed by FG from the control-crossed parent trees identified in the Radiata Pine Breeding Company programme (Dungey *et al.*, 2009), which represent a subset of the genetic entities in New Zealand's deployment population available to forest growers. The clones were selected for the following traits: improved growth rate; stem form; and wood properties (i.e. corewood stiffness and wood density). Clonal stoolbeds were established from somatic seedlings ('emblings'), and stem cutting technology was used for propagating these clones. For the experiment, 12 uniform ramets of each genotype were potted individually in 4 litre plastic pots in the spring prior to the beginning of the experiment. The potting mix contained 15% bark at 5–15 mm, 50% pine A Grade fines, 15% cocoa fibre—coir, and 20% pumice at 7 mm. Plants were grown in a glasshouse in Christchurch, New Zealand (43°33'S, 172°0047'E) where daytime average temperature was 20±5 °C and relative humidity was 50±5%. Plants were fertilized at the beginning of the growing season with a commercial slow-release fertilizer (18:18:18 N:P:K), and watered three times per week by sprinkler irrigation during the whole experiment, which lasted 1 year.

Twelve plants of each genotype were used for the experiment, six in year one (Year1) and six others in year two (Year2). On those plants, hydraulic parameters of roots, stems, and shoots, wood density, plant transpiration, leaf gas exchange, and plant biomass partitioning were measured in summer (January) of Year1. As hydraulic measurements were destructive, these plants were replaced by six other plants. On this second set of six plants per genotype, the gas exchange parameters were re-measured in winter (June) of Year1 and in summer of Year2 and, because wood density determination is also destructive, it was only remeasured in summer of Year2. For measurements in Year1, the plants across all clones had an average height of 52.72±1.48 cm and a basal stem diameter of 0.60±0.01 cm. In Year2, average height was 116.72±2.31 cm and the average basal stem diameter 1.02±0.02 cm. The measured parameters were grouped for subsequent statistical analyses as follows. (i) Hydraulic traits (HT) which included plant, root, and shoot hydraulic conductance (K_{plant}, K_{root}, and K_{shoot}, respectively) as well as stem hydraulic conductivity of the basal and middle position of the stem ($k_{basal\text{-}stem}$ and $k_{middle\text{-}stem}$, respectively). (ii) Normalized hydraulic traits (NHT), which refer to hydraulic efficiency and included leaf-specific plant and leaf-specific shoot hydraulic conductance ($K_{plant\text{-}l}$ and $K_{shoot\text{-}l}$, respectively), root-specific root hydraulic conductance ($K_{root\text{-}r}$), and sapwood-specific conductivity of the basal and middle position of the stem ($k_{basal\text{-}stem\text{-}sw}$ and $k_{middle\text{-}stem\text{-}sw}$, respectively). (iv) Gas exchange (GE) that included all the measurements of net leaf CO_2 assimilation (A), transpiration rate (E), and stomatal conductance (g_s). (4) Wood density (WD) that included all the measurements of wood density (D) in the basal, medium, and top part of the stem in Year1 and Year2. (v) Plant growth rate (PG) that included plant, stem, needle, root, and diameter growth rate (Pgr, Sgr, Ngr, Rgr, and Dgr, respectively). A summary of the measurements performed, their abbreviations, and units is shown in Supplementary Table S1.

Root, shoot, and whole-plant hydraulic conductance and stem conductivity

Root and shoot hydraulic conductance (K_{root} and K_{shoot}) as well as stem hydraulic conductivity of the basal and middle position of the stem ($k_{basal\text{-}stem}$ and $k_{middle\text{-}stem}$) were measured using a high conductance flow meter (HCFM) (Dynamax Inc., Houston, TX, USA). Measurements at the whole-tree level provide important information on the partitioning of resistance along the hydraulic pathway from soil to leaf. Clonal material used for the experiment could differ from naturally germinating seedlings in the root–shoot hydraulic junction. However, this constriction may not be an important component of the total resistance of the water pathway (Tyree and Ewers, 1991). For each genotype, hydraulic parameters were determined in six individual plants per clone. To minimize the potential impact of diurnal periodicity on hydraulic conductance (Tsuda and Tyree, 2000), all measurements were taken between 10.00 h and 14.00 h at ambient temperature inside the glasshouse where the plants were kept during the experiment.

Values of K_{root} and K_{shoot} for a given plant were obtained from the same plant. To measure K_{root} and K_{shoot}, the plants were cut at 5 cm above the soil surface and the cut ends of the shoots and roots were connected to the HCFM. This equipment perfuses degassed water through the root or shoot system or through stem segments by applying pressure to a water-filled bladder contained within the unit. The flow rate of water through the root or shoot was determined using the HCFM under transient mode (Tyree *et al.*, 1995; Bogeat-Triboulot *et al.*, 2002), with flow measured under increasing pressure applied by a nitrogen gas cylinder. The applied pressure was gradually increased from 0 kPa to 500 kPa over the course of ~1 min and the flow rate logged every 2 s using the Dynamax software. Once the transient curve was constructed, hydraulic conductance (K) was calculated using the formula: $K = Q_v/P$, where Q_v is the volumetric flow rate (kg s^{-1}) and P is the applied pressure (MPa). Temperature was automatically recorded by the HCFM and all conductance measurements were corrected to values at 25 °C. Because the HCFM operates under high pressure, the measured K_{root} and K_{shoot} represent maximum values of conductance; that is, in the absence of embolized conduits. After determining K_{root} and K_{shoot}, whole-plant hydraulic conductance was calculated as in Domec *et al.* (2016):

$$1/K_{plant} = 1/K_{root} + 1/K_{shoot} \quad (1)$$

Shoot and root contribution to the whole-plant conductance was evaluated through the K_{root}/K_{shoot} ratio (Rodríguez-Gamir *et al.*, 2016).

Stem hydraulic conductance was measured in stem segments from the basal and middle part of the stem. The stems were ~6 cm long. Stem segment length was measured for calculating stem conductivity for each of the two stem segments of each plant ($k_{basal\text{-}stem}$ and $k_{middle\text{-}stem}$, respectively).

Normalized hydraulic traits

After the hydraulic conductance measurements, all plant fractions were dried in a forced-draft oven at 75 °C for 72 h and weighed. Also, the xylem diameter of the stem segments used for $k_{basal\text{-}stem}$ and $k_{middle\text{-}stem}$ measurements was determined. K_{plant}, K_{root}, and K_{shoot} were normalized by dry biomass. Root-specific root hydraulic conductance ($K_{root\text{-}r}$) was calculated by dividing K_{root} by the root dry weight. Leaf-specific shoot

and leaf-specific plant hydraulic conductance ($K_{shoot\text{-}l}$ and $K_{plant\text{-}l}$, respectively) were obtained by dividing K_{shoot} and K_{plant}, respectively, by the total leaf biomass. Sapwood-specific conductivity of the basal and middle part of the stem ($k_{basal\text{-}stem\text{-}sw}$ and $k_{middle\text{-}stem\text{-}sw}$, respectively) was calculated by dividing $k_{basal\text{-}stem}$ or $k_{middle\text{-}stem}$ by the xylem cross-sectional area of the stem segments.

Net leaf CO_2 assimilation, transpiration rate, and stomatal conductance

Net leaf CO_2 assimilation (A), transpiration rate (E), and stomatal conductance (g_s) were measured in January of Year1 ($A_{JanYear1}$, $g_{sJanYear1}$, $E_{JanYear1}$), in June of Year1 ($A_{JunYear1}$, $g_{sJunYear1}$, $E_{JunYear1}$), and in January of Year2 ($A_{JanYear2}$, $g_{sJanYear2}$ and $E_{JanYear2}$). At each sampling time, A, g_s, and E were determined on six individual plants for each genotype. Measurements were made with a portable photosynthesis system (Model LI-6400XT, Li-Cor, Lincoln, NE, USA) equipped with a light source. For each tree, three fascicles taken from the central part of each plant were placed across the 2×3 cm cuvette to avoid shading between needles. Temperature in the cuvette was maintained at 20 °C, while the leaf-to-air vapour pressure deficit (VPD) was maintained at ~1 kPa to limit its negative effect on g_s (Oren *et al.*, 1999). The needles were left to equilibrate at a CO_2 concentration of 400 µmol mol^{-1} and saturating irradiance (1500 µmol m^{-2} s^{-1}). Measurements were recorded after the values of g_s were stable. The measurements were taken between 10.00 h and 14.00 h. All measurements were presented on a surface area basis. The foliage surface area of the fascicules used for each measurement was calculated for fascicles consisting of three needles by: $S=[d\ l(3+\pi)]/2$, where S is the fascicle surface included in the Li-Cor cuvette, d is the fascicle diameter, and l is the length of the needle segment clipped in the cuvette (3 cm) (Bown *et al.*, 2009).

Wood density

In January of Year1, wood density was measured on the same stems that were used for the hydraulic measurements in the basal and middle sections of the stem (D_{bYear1} and D_{mYear1}, respectively). In January of Year2, wood density was determined in the basal, middle, and top part of the stem (D_{bYear2}, D_{mYear2}, and D_{tYear2}, respectively). Bark of 3 cm long stem segments was removed with a razor blade, and the fresh volume of the stem (including the pith) was determined by Archimedes' principle (Hacke *et al.*, 2000). Samples were dried at 75 °C for 72 h and weighed. Wood density was calculated as the ratio of dry weight to fresh volume.

Whole-plant transpiration

Before measuring hydraulic conductance, whole daily plant transpiration (T_p) was measured in January of Year1. To measure T_p, the pots were covered with plastic sheets. T_p of each plant was calculated as the difference between the weight of the watered pot (after draining) and the weight of the pot after 24 h of being watered. The mean of three determinations on each plant (one per day during three consecutive days) was considered as representative of each individual plant (Rodríguez-Gamir *et al.*, 2016).

Plant growth rate

In January of Year1 and January of Year2, stem diameter was measured and, after harvest, plant biomass was dried in a forced-draft oven at 75 °C for 72 h to obtain the dry weight biomass (DW) of all the plant fractions. Plant, stem, needles, root, and diameter growth rate (Pgr, Sgr, Ngr, Rgr, and Dgr, respectively) were calculated as in Fichot *et al.* (2011):

$$Pgr = (Plant\ DW_{Year2} - Plant\ DW_{Year\ 1})\ /Plant\ DW_{Year1} \quad (2)$$

$$Sgr = (Stem\ DW_{Year2} - Stem\ DW_{Year\ 1})\ /Stem\ DW_{Year1} \quad (3)$$

$$Ngr = (Needles\ DW_{Year2} - Needles\ DW_{Year\ 1})\ /Needles\ DW_{Year1} \quad (4)$$

$$Rgr = (Root\ DW_{Year2} - Root\ DW_{Year\ 1})\ /Root\ DW_{Year1} \quad (5)$$

$$Dgr = (Stem\ diameter_{Year2} - Stem\ diameter_{Year\ 1})\ /Stem\ diameter_{Year1} \quad (6)$$

Statistical analysis

All variables were checked for normality. ANOVAs were used to test for significant differences among clones for a given variable. Linear regression analysis and Pearson correlation coefficients were used to quantify the association between pairs of variables. For each of the five groups (i.e. HT, NHT, GE, WD, and PG), one principal component analysis (PCA) was performed, with all the descriptors included in the group (Supplementary Table S1), in order to summarize the data and calculate five new variables for each plant of the experiment (HT_{index}, NHT_{index}, GE_{index}, WD_{index}, and PG_{index}). PCA seeks linear projections of the original data to a lower dimensional space while capturing major variability of the original data and is often used to reduce the dimensionality of large data sets, by transforming a large set of variables into a smaller one that still contains most of the information in the large set (Jolliffe, 1986). Therefore, for our data, each index integrated all the measured parameters of each group in a single value for each individual plant. As index for each plant, the axis score on the first axis of the respective PCAs was used. A sixth PCA was performed using the parameters, HT_{index}, NHT_{index}, K_{root}/K_{shoot}, T_p, GE_{index}, WD_{index}, and PG_{index}. All the PCAs were performed with individual data for each plant. Note that each plant harvested in January of Year1 was replaced by a similar plant for the measurements recorded in June of Year1 and January of Year2.

Results

Variation among clones

Significant variations in all the hydraulic traits, normalized hydraulic traits, gas exchange parameters, wood density, and growth rate indicators were found among the studied genotypes (Figs 1, 2). The respective descriptors belonging to the groups HT, NHT, GE, WD, and PG were highly intercorrelated (Supplementary Table S2). For the PCA performed for HT (Supplementary Fig. S1), the first and second axes explained 84.5% and 10.1% of the total variance, respectively; 77.7% and 11.3% for the NHT PCA; 91.1% and 2.8% for the GE PCA; 82.3% and 6.4% for the WD PCA; and 83.3% and 5.4% for the PG PCA. The axis scores for each plant on the first axis of each PCA were used as new variables that represented integrated measures of HT, NHT, GE, WD, or PG and named HT_{index}, NHT_{index}, GE_{index}, WD_{index}, and PG_{index}.

Hydraulic and normalized hydraulic traits

For all the clones, K_{root} was significantly greater ($P<0.01$) than K_{shoot} (Fig. 1A). Larger relative differences between K_{root} and

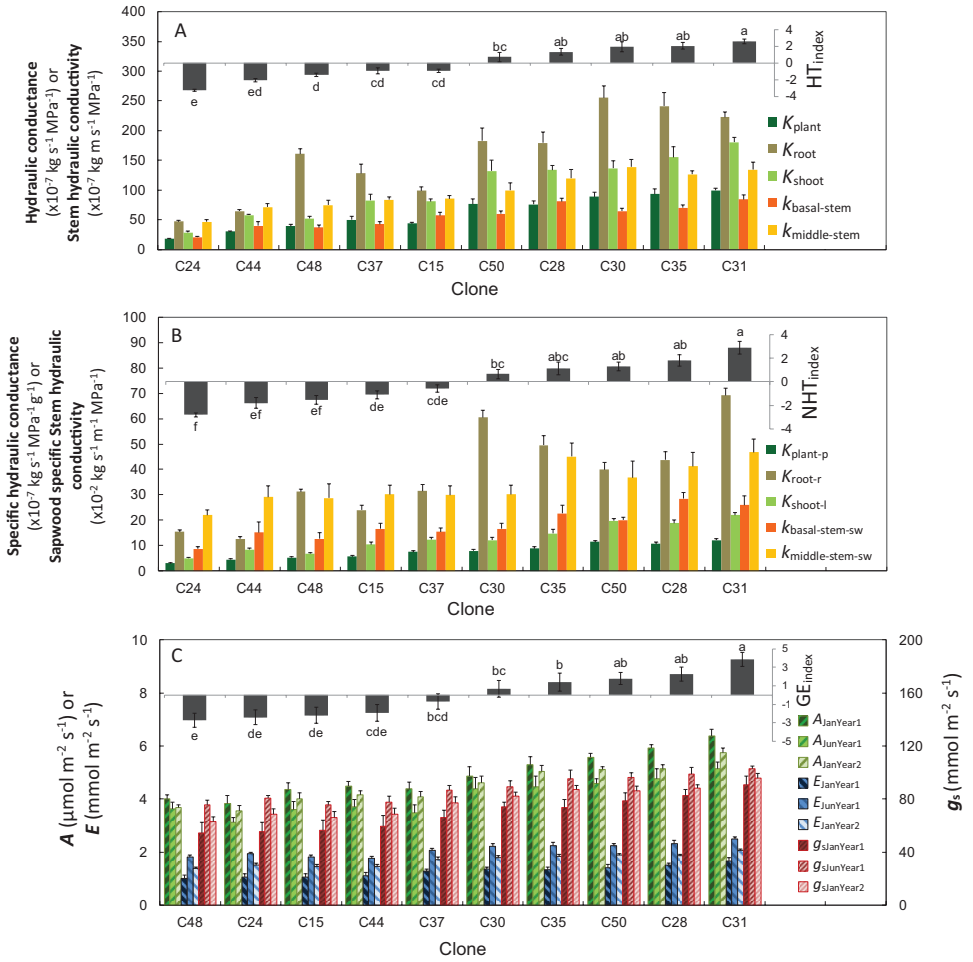

Fig. 1. The values of hydraulic traits (HT), normalized hydraulic traits (NIT), and gas exchange (GE) measurements. Average values of (A) whole-plant hydraulic conductance (K_{plant}), root hydraulic conductance (K_{root}), shoot hydraulic conductance (K_{shoot}), hydraulic conductivity of the basal part of the stem ($k_{basal\text{-}stem}$), hydraulic conductivity of the middle part of the stem ($k_{middle\text{-}stem}$), and hydraulic traits index (HT_{index}); (B) leaf-specific plant hydraulic conductance ($K_{plant\text{-}l}$), root-specific root hydraulic conductance ($K_{root\text{-}r}$), leaf-specific shoot hydraulic conductance ($K_{shoot\text{-}l}$), sapwood-specific conductivity of the basal part of the stem ($k_{basal\text{-}stem\text{-}sw}$), sapwood-specific conductivity of the middle part of the stem ($k_{middle\text{-}stem\text{-}sw}$), and normalized hydraulic traits index (NHT_{index}); and (C) net CO_2 assimilation (A), transpiration rate (E), and stomatal conductance (g_s) in January of Year1 ($_{JanYear1}$), June of Year1 ($_{JunYear1}$), and January of Year2 ($_{JanYear2}$), and gas exchange index (GE_{index}) for the 10 *P. radiata* genotypes (C15, C24, C28, C30, C31, C35, C37, C44, C48, and C50). Values are means ±SE (n=6). Different letters indicate statistically significant differences in HT_{index}, NHT_{index}, and GE_{index} between clones.

K_{shoot} were found in clones 48, 30, and 24 that presented the greater values of K_{root}/K_{shoot} (3.1 for C48, 1.9 for C30, and 1.7 for C24). For the other seven clones, K_{root}/K_{shoot} ranged between 1.1 and 1.6. Regarding stem hydraulics, $k_{middle\text{-}stem}$ was greater (P<0.001) than $k_{basal\text{-}stem}$ for all clones (Fig. 1A) and $k_{middle\text{-}stem\text{-}sw}$ was higher (P<0.001) than $k_{basal\text{-}stem\text{-}sw}$ (Fig. 1B).

Increasing values of the HT_{index} obtained by the HT PCA reflected greater values of K_{plant}, K_{root}, K_{shoot}, $k_{basal\text{-}stem}$, and $k_{middle\text{-}stem}$ (Fig. 1A). Likewise, increasing values of the NHT_{index} were related to increasing values of $K_{plant\text{-}l}$, $K_{shoot\text{-}l}$, $K_{root\text{-}r}$, $k_{basal\text{-}stem\text{-}sw}$, and $k_{middle\text{-}stem\text{-}sw}$ (Fig. 1B). There were significant differences (P<0.01) between clones for the HT_{index} and NHT_{index}. The HT_{index} was significantly lower in C24 and C44, and greater in C28, C30, C35, and C31 (Fig. 1A). The NHT_{index} was lower in C24, C44, and C48, and greater in C35, C50, C28, and C31 (Fig. 1B).

Strong positive correlations existed between all hydraulic parameters (K_{plant}, K_{root}, K_{shoot}, $k_{basal\text{-}stem}$, and $k_{middle\text{-}stem}$) (see Pearson correlation matrix in Supplementary Table S2 and Fig. 3A–C). Similarly, a large positive correlation was found between all the normalized hydraulic traits ($K_{plant\text{-}l}$, $K_{root\text{-}r}$, $K_{shoot\text{-}l}$, $k_{basal\text{-}stem\text{-}sw}$, and $k_{middle\text{-}stem\text{-}sw}$; Supplementary Table S2; Fig. 3D–F).

Gas exchange

For all the gas exchange parameters (A, E, and g_s; Fig. 1C), two-way ANOVAs were performed for each parameter, with clone, date, and clone×date as factors. The factors clone and date were statistically significant (P<0.001) but not the interaction clone×date (P>0.05). Strong correlation was found between all the gas exchange parameters (Supplementary Table

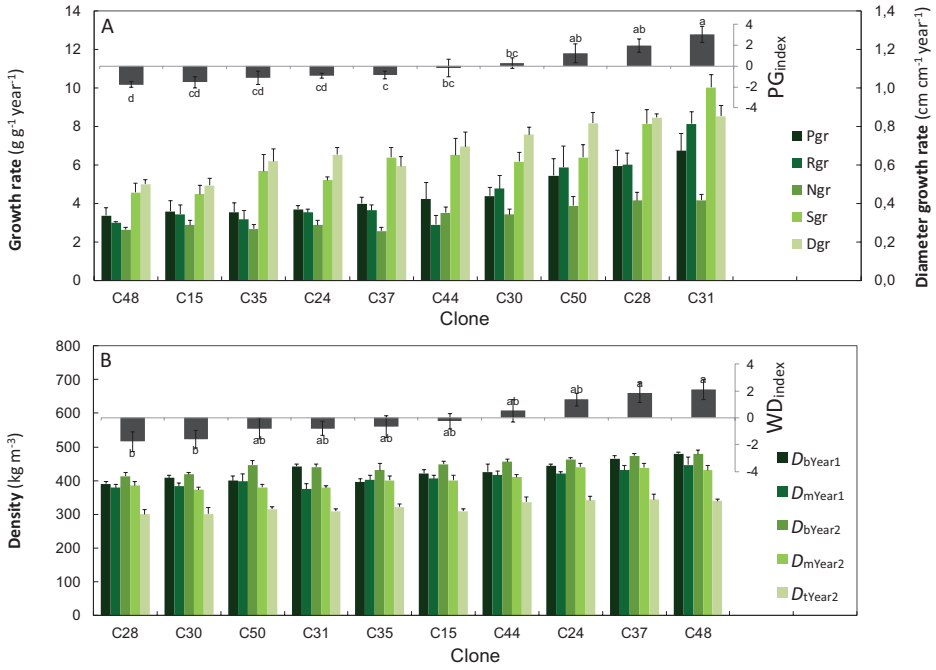

Fig. 2. Determination of growth rates and wood density. Average values of (A) plant growth rate (Pgr), root growth rate (Rgr), needle growth rate (Ngr), stem growth rate (Sgr), diameter growth rate (Dgr), and plant growth rate index (PG_{index}), and (B) wood density in the base, middle, or top position of the stem in Year1 and Year2 (D_{bYear1}, D_{mYear1}, D_{bYear2}, D_{mYear2}, and D_{tYear2}) and wood density index (WD_{index}) for the 10 *P. radiata* genotypes (C15, C24, C28, C30, C31, C35, C37, C44, C48, and C50). Values are means ±SE (n=6). Different letters indicate statistically significant differences in PG_{index} and WD_{index} between clones.

S2). A greater GE_{index} was related to increasing values of A, E, and g_s (Fig. 1C), and was significantly greater (P<0.01) for C31, C28, and C50, and lower for C48, C24, C15, and C37.

Plant growth

Total plant biomass in the summer of Year1 differed between clones (P<0.01) (Fig. 4). Total plant dry weight ranged between 14 g and 20 g DW. However, there were no statistically differences (P>0.05) in stem DW between clones, with an average value of 0.5 g DW. Larger differences in plant biomass between clones were found after 1 year of growth (summer of Year2). At that moment, C31 had the largest total plant DW (115.4 g) and stem DW biomass (50.1 g), and C24 had the lowest (57.9 g of plant DW and 21.5 g of stem DW). Thus, Pgr, Sgr, Rgr, Ngr, and Dgr differed markedly between clones (Fig. 2A). Greater PG_{index} was related to increasing values of Pgr, Sgr, Rgr, Ngr, and Dgr. This index was statistically significantly greater (P<0.001) for C31, C28, and C50, and lower for C48, C15, C35, and C24.

Wood density

Strong correlations were found between all the density measurements (see the Pearson correlation matrix in Supplementary Table S2). For each clone, greater WD_{index} was related to greater density for all the parts of the stem at each date of sampling (Fig. 2B). The ANOVA considering clone as the only factor showed statistically significant clonal differences (P<0.001) for wood density. C28 had the lowest density (373.5 kg m^{-3}), while C48 had the heaviest (434.9 kg m^{-3}). The two-way ANOVAs showed that the wood density decreased significantly from the base to the top of the stem both in Year1 and in Year2 (Table 1). Averaged across all the clones, mean wood density in Year1 was 427.3 kg m^{-3} at the base of the stem and 405.8 kg m^{-3} in the middle. The gradient observed in Year2 was 447.1 kg m^{-3} at the base, 403.9 kg m^{-3} in the middle, and 321.8 kg m^{-3} at the top.

Interactions between the factors

The PCA performed for the variables PG_{index}, WD_{index}, HT_{index}, NHT_{index}, GE_{index}, K_{root}/K_{shoot}, and T_p explained 81.79% of the total variance of the data (Fig. 5). In the first axis, NHT_{index}, GE_{index}, and PG_{index} had highly positive factor loadings, and WD_{index} had highly negative factor loading. Positive values of the second axis were mainly associated with increasing K_{root}/K_{shoot} and increasing T_p. The PCA clearly separated the clones having more extreme values for the analysed variables. Specifically, C24 was in the left lower quadrant, reflecting their low values for HT_{index}, NHT_{index}, GE_{index}, and PG_{index}, and their high value for WD_{index}. C28 and C31 were in the right side of the plot with high values of NHT_{index}, GE_{index}, and PG_{index},

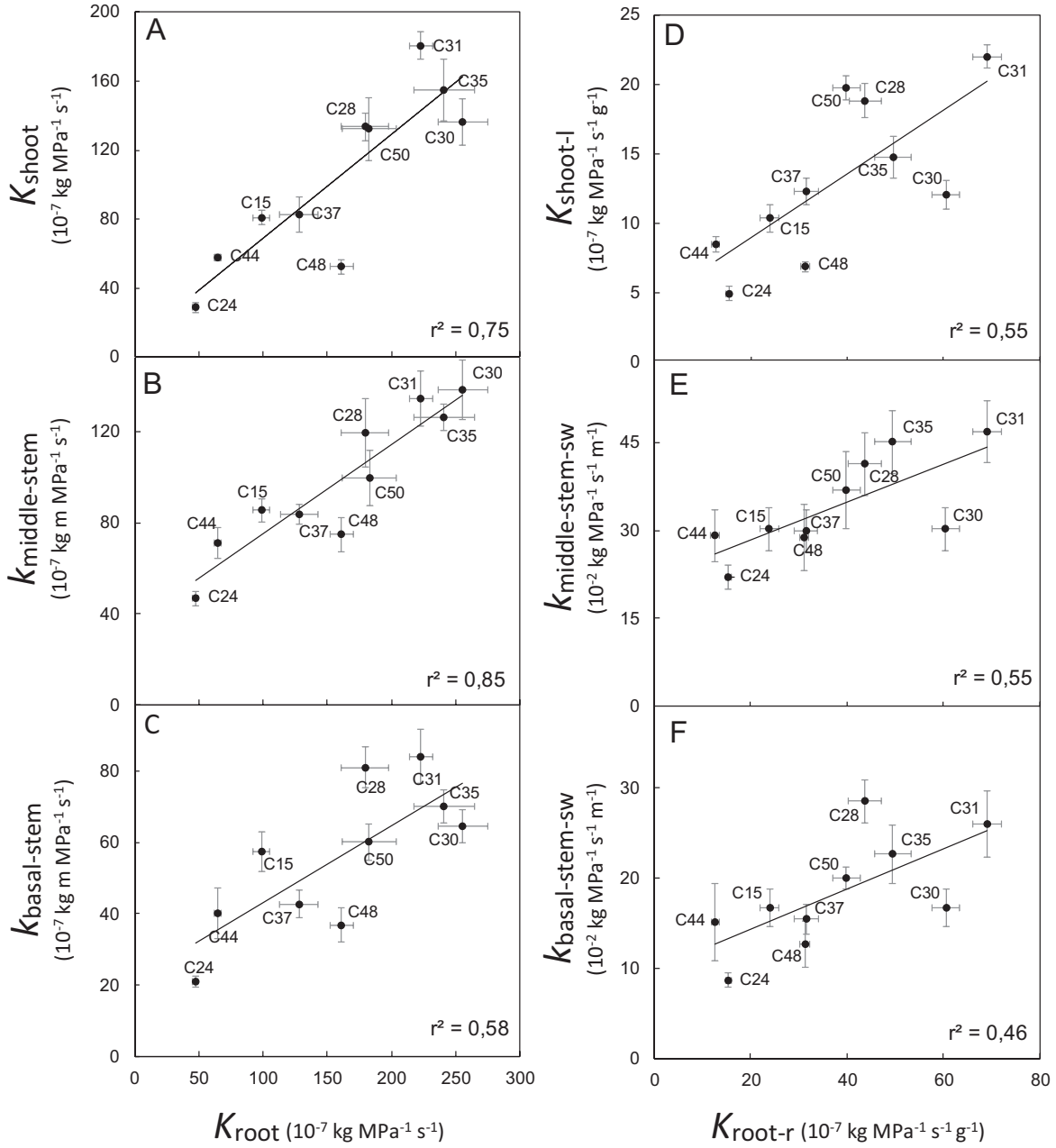

Fig. 3. Linear relationships between different parts of the plant hydraulic system. Relationship of (A) shoot hydraulic conductance (K_{shoot}), (B) hydraulic conductivity of the middle part of the stem ($k_{middle\text{-}stem}$), and (C) hydraulic conductivity of the basal part of the stem ($k_{basal\text{-}stem}$) to root hydraulic conductance (K_{root}), and of (D) leaf-specific shoot hydraulic conductance ($K_{shoot\text{-}l}$), (E) sapwood-specific hydraulic conductivity of the middle part of the stem ($k_{middle\text{-}stem\text{-}sw}$), and (F) sapwood-specific hydraulic conductivity of the basal part of the stem ($k_{basal\text{-}stem\text{-}sw}$) to root-specific root hydraulic conductance ($K_{root\text{-}r}$). Each point represents the mean (±SE, n=6) value of these parameters for each different *P. radiata* genotype used in the experiment (C15, C24, C28, C30, C31, C35, C37, C44, C48, and C50).

and low values of WD_{index}. C48 was in the upper left quadrant with high K_{root}/K_{shoot} and WD_{index}, and low PG_{index}, GE_{index}, NHT_{index}, and HT_{index}.

The position of the eigenvectors for each variable showed strong positive relationships between T_p and HT_{index} (see Pearson correlation in Table 2). T_p, that ranged from 5.1 g d^{-1} (for clone C24) to 11.1 g d^{-1} (for C30), was linearly related to K_{plant} (Fig. 6A). Similarly, the correlation between PG_{index}, GE_{index}, and NHT_{index} was evident in the linear relationships found between Pgr, A, E, and $K_{plant\text{-}l}$ (Fig. 6B, C).

WD_{index} had a strong negative correlation with PG_{index}, GE_{index}, NHT_{index}, and HT_{index} (Table 2). The larger relative

contribution of the root to the total plant hydraulic conductance (higher K_{root}/K_{shoot} ratio) was negatively related to NHT_{index}, GE_{index}, and PG_{index} (Table 2).

A strong negative correlation was found between wood density and sapwood-specific stem conductivity (Fig. 7A). This relationship was very consistent since the regression combined the data from both the basal and the middle position of the stem. A small reduction in wood density translated into a large increase in sapwood-specific stem conductivity. Similarly, Sgr was negatively related to wood density at all plant heights (Fig. 7B). Reductions of 9.6, 10.6, and 9.6 kg m^{-3} of wood density in the basal, middle, and top position of the stem, respectively, were calculated per unit of Sgr increment.

Discussion

This study clearly showed interclonal variation for hydraulic, photosynthetic, growth, and wood density traits (Figs 1, 2), and strong coordination and trade-offs between them. To our knowledge, few studies have addressed all these relationships together within a given species. The interclonal variation of these characters and the coordination between them allow selection of genotypes for the commercial forestry sector based on their hydraulic properties, gas exchange behaviour, wood characteristics, and productivity. These characters will be related to different management strategies of this species and selecting genotypes that are most suitable for individual sites that are water limited (Rodríguez-Gamir *et al.*, 2019), have water sensitive watersheds (Meason *et al.*, 2019), or are more likely to experience drier and more extreme climatic conditions with climate change.

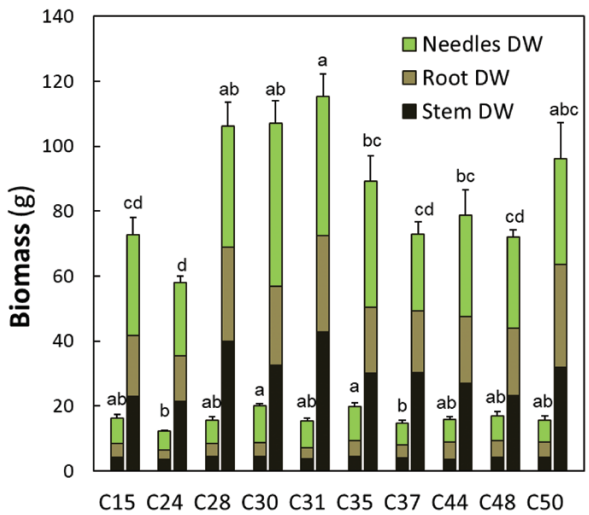

Fig. 4. Biomass partitioning. Biomass partitioning (DW of root, stem, and needles) for the 10 clones (C15, C24, C28, C30, C31, C35, C37, C44, C48, and C50) in January of Year1 (left column for each clone) and in January of Year2 (right column for each clone). Values are means of six plants for each clone and date. Error bars represent the SE for plant DW. Different letters indicate statistically significant differences in plant DW between the clones for each date.

Hydraulic efficiency is related to plant growth and gas exchange

Plant water transport was a function of whole-plant hydraulic capacity (K_{plant}; Fig. 6A). This result highlighted the intrinsic importance of the total hydraulic system in regulating water transport within the plant (Tsuda and Tyree, 2000; Rodríguez-Gamir *et al.*, 2016), and thus gas exchange and carbon allocation.

Hydraulic efficiency (normalized hydraulic conductance), growth, and leaf-specific gas exchange were found to be intimately linked (Figs 5, 6B, C; Table 2). The hydraulic–photosynthesis coordination in woody species has been often demonstrated comparing different species, for example species of subtropical forest (Zhu *et al.*, 2013) or temperate woody species (Sack *et al.*, 2003). However, within a species, this link has commonly been quantified by (i) the artificial modification of $K_{plant-l}$, for example physically damaging the plant with defoliation, stem notching, or root pruning (Meinzer and Grantz, 1990; Sperry *et al.*, 1993; Pataki *et al.*, 1998; Hubbard *et al.*, 2001; Cochard *et al.*, 2002); (ii) in response to stress (Domec *et al.*, 2009); or (iii) by altering growing conditions (sun/shade) (Pratt *et al.*, 2012). Without these artefacts, our work demonstrated that the hydraulic processes at the whole-plant scale explained the variation in gas exchange parameters between the *P. radiata* clones. Our study supported the prediction from a theoretical model that the intercellular CO_2 concentration required for photosynthesis should be strongly dependent on plant hydraulic conductance (Katul *et al.*, 2003). Thus, equilibrium between maximum carbon demand by photosynthesis and maximum water supply leads to a constant long-term mean intercellular CO_2 concentration. In addition, trees when they grow maintain a relatively constant $K_{plant-l}$, so that the amount of water delivered by the conducting system per unit of leaf area is maintained with increased tree size (Zhang *et al.*, 2009). The occurrence of these apparently co-evolutionary traits supports the fact that the control and strong interdependency of the hydraulic and biochemical plant properties are manifested at the genotype level. Therefore, high $K_{plant-l}$ and high A are required when predicting growth characteristics of different clones of *P. radiata* (Figs 5, 6B, C). These conditions are necessary for high productivity in forest trees (Tyree *et al.*, 1998).

Hydraulic partitioning

We found strong evidence of hydraulic coordination between the root, shoot, and stem (Fig. 3), and that the individual hydraulic traits were highly correlated with the whole-plant hydraulic system (Supplementary Table S2). For example, genotypes with high K_{root-r} also had high $k_{stem-sw}$ and $K_{shoot-l}$.

Table 1. ANOVA results for wood density in January of Year1 and January of Year2 using clone and stem position as factors

	January Year1		January Year2	
	df	***F*-value and significance**	**df**	***F*-value and significance**
Factor				
clone	9	7.35***	9	9.79***
position	1	13.75***	2	313.84***
clone×position	9	1.5ns	18	0.59ns
Residuals	100		150	

n=6 for each clone×position combination; ***P<0.001; ns, non-significant.

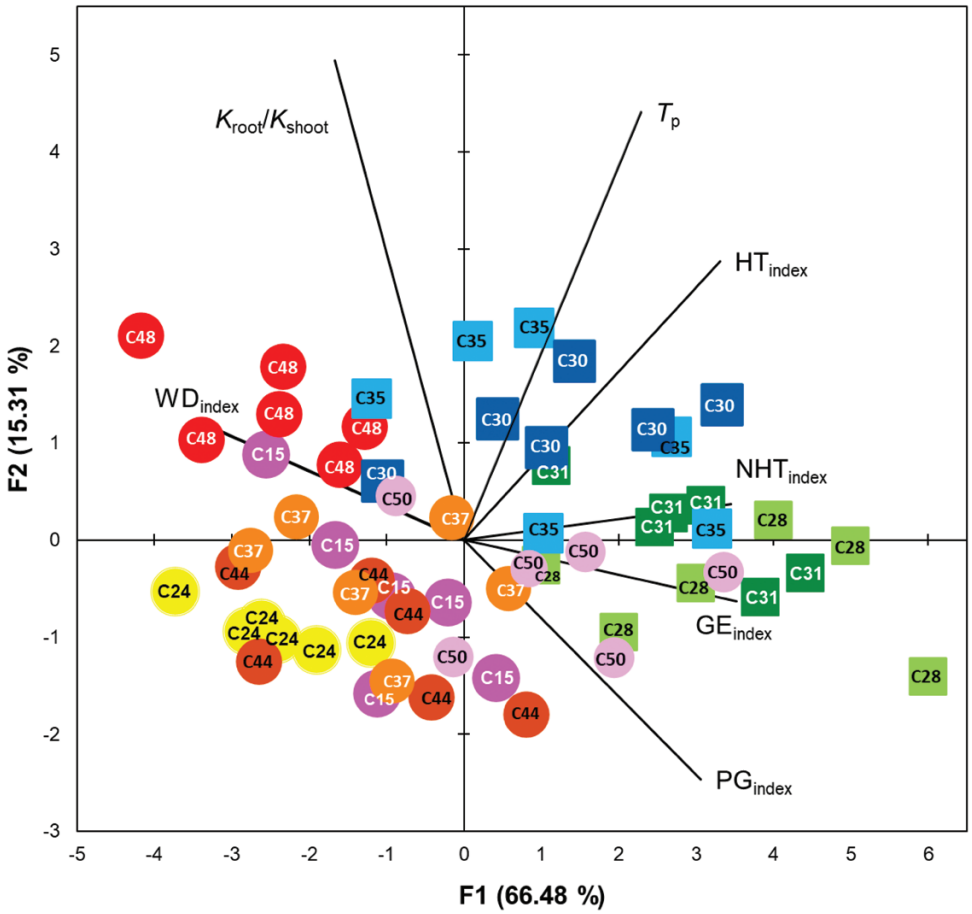

Fig. 5. Principal components analysis (PCA). PCA for the wood density index (WD_{index}), hydraulic traits index (HT_{index}), normalized hydraulic traits index (NHT_{index}), gas exchange index (GE_{index}), plant growth rate index (PG_{index}), daily whole-plant transpiration (T_p), and root hydraulic conductance/shoot hydraulic conductance ratio (K_{root}/K_{shoot}). Each point in the plot represents an individual tree for each clone.

This suggests that hydraulics traits of a given organ could be proportionally scaled by the hydraulic traits of another plant organ or whole plant (Sack *et al.*, 2003, Pratt *et al.*, 2010; Nolf *et al.*, 2015; Rodríguez-Gamir *et al.*, 2019). This would explain why many studies have related hydraulic conductance traits at organ level to tree growth rates (Tyree *et al.*, 1991; Fan *et al.*, 2012) or gas exchange parameters (Brodribb and Feild, 2000; Aasamaa and Sõber 2001; Clearwater and Meinzer, 2001; Sack *et al.*, 2003; Brodribb *et al.*, 2005).

Few studies have investigated the interaction between the whole-root system and whole-shoot system hydraulics (Domec *et al.*, 2009; Johnson *et al.*, 2016). We found a linear relationship between K_{root} and K_{shoot} (Fig. 3A), with an average ratio K_{root}/K_{shoot}=1.6 when considering all the clones, with K_{root} being higher than K_{shoot} in all of them (Fig. 1A). Tyree *et al.* (1998) found the K_{root}/K_{shoot} ratio values for five different neotropical tree species were also close to one. Supporting this, stem hydraulic conductivity was higher in roots than in stems

Table 2. Pearson correlation coefficients between NHT_{index}, GE_{index}, PG_{index}, HT_{index}, WD_{index}, T_p, and K_{root}/K_{shoot} based on measurements obtained from 36 trees

	NHT_{index}	GE_{index}	PG_{index}	HT_{index}	WD_{index}	T_p	K_{root}/K_{shoot}
NHT_{index}	1						
GE_{index}	0.93***	1					
PG_{index}	0.79***	0.85***	1				
HT_{index}	0.88***	0.82***	0.60***	1			
WD_{index}	–0.72***	–0.82***	–0.72***	–0.69***	1		
T_p	0.51***	0.48***	0.25*	0.78***	–0.43**	1	
K_{root}/K_{shoot}	–0,31**	–0.40**	–0.40**	–0.21ns	0.42**	–0.14ns	1

***P<0.001; **P<0.01; *P<0.05; ns, non-significant.

in nine woody species (Martínez-Vilalta *et al.*, 2002) and in *Sassafras albidum* and *Rhus typhina* (Jaquish and Ewers, 2001). However, these studies measured conductivity in root and stem segments, which did not allow evaluation of the contribution of the root or the stem to the complete hydraulic system of the plant. We can assume that the partitioning of hydraulic conductance represents the trade-off between transport water efficiency and hydraulic safety at the scale of the whole plant (Drake *et al.*, 2015; Johnson *et al.*, 2016). Avoidance of cavitation is well established as a dominant factor driving the evolution of the xylem structure and function, and is a key trait that determines a woody plant's ability to survive water stress (Tyree and Zimmermann, 2002; Pratt *et al.*, 2008; Kursar *et al.*, 2009). However, it has been suggested that for conifers, the evolution of water transport efficiency is independent of the evolution of protection mechanisms against hydraulic failure (Piñol and Sala, 2000; Martínez-Vilalta *et al.*, 2009). Therefore, other mechanisms should be involved in conifer evolution for avoiding embolism. Water stored within the plant can be mobilized to alleviate the risk of embolism (Salleo *et al.*, 2009; Pfautsch *et al.*, 2015, Rosner *et al.*, 2019). Several water storage locations exist within conifers, including the sapwood, cell walls, elastic tissues of the bark (i.e. cambium, phloem, and parenchyma), and needle mesophylls (Zimmermann, 1983). The stem-mediated hydraulic redistribution is the result of a complex interplay of competing water potential gradients inside the tree when it is exposed to soil water limitation. Under soil water-limiting conditions, the tension in the dry root becomes an increasingly important driving force for the water flow coming from the part of the plant with increased water potential (Pfautsch *et al.*, 2015). So, when the tensions above-ground and below-ground are similar under water stress, water tends to flow to the path with the least resistance (Nadezhdina *et al.*, 2009), which would be towards the root system which has major hydraulic conductance. This hypothesis is supported by the results of this study as the K_{root}/K_{shoot} showed a negative effect, limiting the total K_{plant} and, therefore, photosynthesis and growth as well (Fig. 5). From an adaptive perspective, it would be unnecessary to maintain a plant functional trait limiting growth and gas exchange. So, its function as a cavitation-avoiding mechanism could be justified (Rodríguez-Gamir *et al.*, 2016).

Wood density as a key part of water transport and leaf function

There was a decreasing wood density gradient in *P. radiata* from the base to the crown (Figs 2B, 7B). This can be attributed to a gradient in cell wall thickness and related to the maturation state of the stem (Cato *et al.*, 2006). A small decrease in wood density translated into a large increase in sapwood-specific stem conductivity (Fig. 7A) (Stratton *et al.*, 2000; Domec and Gartner, 2003; Bucci *et al.*, 2004, 2005; Pratt *et al.*, 2007; McCulloh et al., 2011, 2015). Therefore, wood density provides an index of the balance between solid material and the relative cross-sectional area available for water transport (Meinzer *et al.*, 2008).

In addition, greater wood density was negatively related to growth rates (Figs 5, 7B) (Muller-Landau, 2004; King *et al.*, 2005; Poorter *et al.*, 2008; Chave *et al.*, 2009; Wright *et al.*, 2010) and gas exchange (Fig. 5; Table 2) (Bucci *et al.*, 2004; Santiago *et al.*, 2004). The negative correlation between wood density and stem growth rate can be related to competition between sinks. In the stem, sink strength (the ability of heterotrophic tissues to use photoassimilates) can be measured as the production of new cells and cell wall thickening (Thomas *et al.*, 2007). In *Pinus* sp., cell wall thickness (determinant factor of density) was negatively related to the rate of cell division (determinant factor of growth), which suggests the existence of mechanisms of competition between the production of new cells and the thickening of the existing cells that finally modulate CO_2 assimilation (Nicholls and Waring, 1977). Supporting this, Conroy *et al.* (1990) observed that *P. radiata* growing at elevated levels of CO_2 increased both biomass production and wood density. Sink strength is a primary factor determining the rate of carbohydrate export from, and ultimately the photosynthetic activity of, the source leaves (Gifford and Evans, 1981; Coruzzi and Bush, 2001). It has been proposed that the coordination between leaf gas exchange and density is probably mediated by the inverse relationship between hydraulic traits and wood density (Meinzer *et al.*, 2008). However, the strong co-variation observed between wood density and gas exchange could be explained by another, not mutually exclusive, mechanism. Cell wall thickness is related to carbohydrate supply (Ford *et al.*,

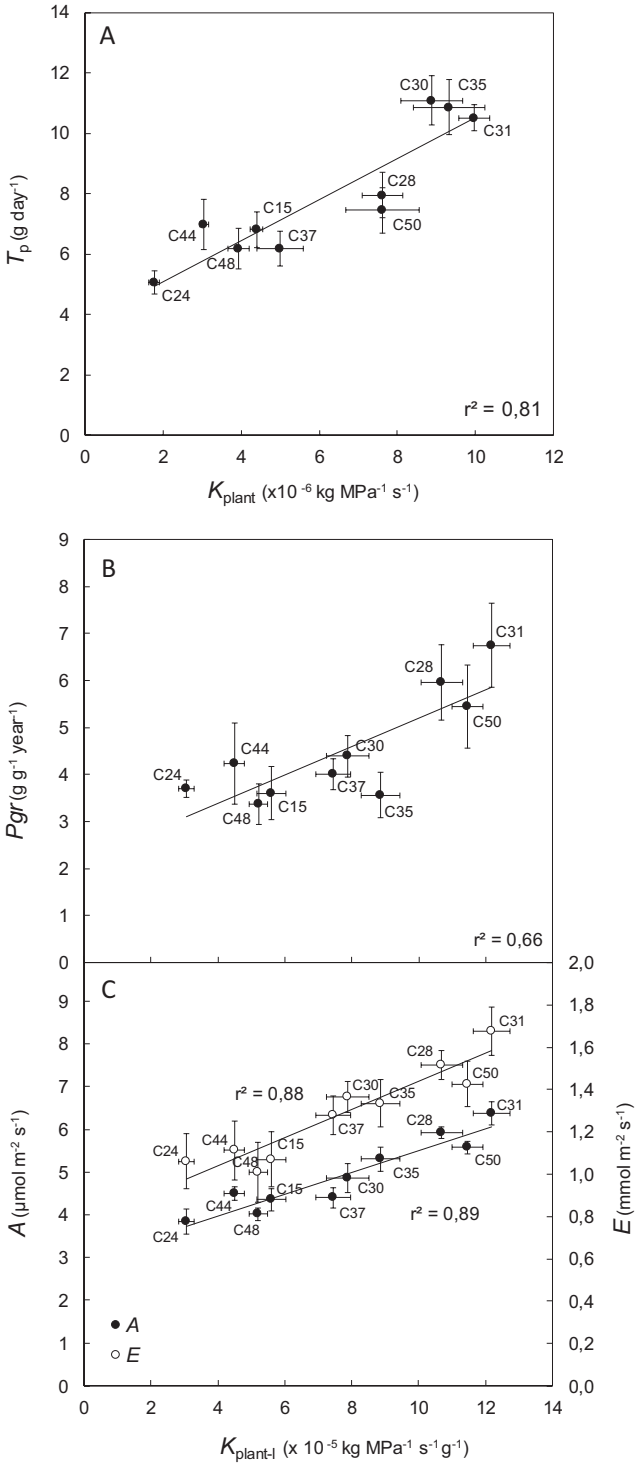

Fig. 6. Influence of the whole-plant hydraulic system on plant daily transpiration, plant growth rate, net CO_2 assimilation. and transpiration rate. Relationship of (A) whole-plant daily transpiration (T_p) and whole-plant hydraulic conductance (K_{plant}), and (B and C) plant growth rate (Pgr), net CO_2 assimilation (*A*), and transpiration rate (*E*) to leaf-specific plant hydraulic conductance ($K_{plant-l}$). Each point represents the mean (±SE, *n*=6) value of these parameters for each different *Pinus radiata* genotype used in the experiment (C15, C24, C28, C30, C31, C35, C37, C44, C48. and C50).

1978). The carbohydrate transport in most plants takes place in the form of sugars. Sugar loading into the phloem and its transport rate through the plant is dependent not only on the photosynthesis rate but also on the xylem water potential (Cernusak *et al.*, 2003), as decreasing xylem water potential limits sugar transport for a given phloem structure because water is held more tightly in the xylem (Hölttä *et al.*, 2009). Considering that the transpiration stream in the xylem is directly connected to phloem tissue (Pfautsch *et al.*, 2015), it is hypothesized that factors that control the building and characteristics of the hydraulic system are interconnected with the synthesis and transport of carbohydrates and therefore with the biochemical reactions that take place in the leaves (Paul and Foyer, 2001; Euring *et al.*, 2014) and that leaf gas exchange regulation is directly connected with sink activity and plant structure (Nikinmaa *et al.*, 2013). Thus, wood density and the building of the hydraulic system are apparently central for understanding how CO_2 assimilation at the leaf level might be integrated with plant hydraulic conductance and growth.

Even though widespread dieback of natural conifer forests from arid habitats is increasing with the occurrence of recent droughts (Sevanto *et al.*, 2014; IUCN, 2019), conifers growing under temperate climates have large hydraulic safety margins owing to their strong stomatal regulation of leaf water status in combination with a rather dense and safe xylem. Stomatal regulation should allow conifers to better acclimate to a progressively higher atmospheric demand due to rising temperatures (Oren *et al.*, 1999; Meinzer, 2002). Wood density represents a weighted representation of the different types of xylem cells involved in water transport and thus, as shown in this study, correlates well with hydraulic traits of tracheid-based species. Conifer species from the *Picea*, *Pinus*, or *Pseudostuga* genera used in large-scale plantations worldwide in general have a dense wood and are more resistant to hydraulic dysfunction than most planted angiosperms, such as species from the *Eucalyptus*, *Populus*, *Salix*, or *Betula* genera (Hacke *et al.*, 2017; McCulloh *et al.*, 2019). In addition, it seems that conifer clones and seedlings, especially at a young age, perform better under drought than angiosperms (Vander Willigen and Pammenter, 1998; Rosner, 2013; Barotto *et al.*, 2018), which renders them less vulnerable to future climate change impact, thus making conifers more suitable to meet our future demand for wood productivity and carbon storage.

Conclusion

This study demonstrated that several relationships and trade-offs between hydraulic properties, gas exchange, plant growth, and wood density can be described at the whole-plant scale and at the clonal level in *P. radiata*. The proportional increase in NHT_{index}, GE_{index}, and PG_{index} with decreasing WD_{index} demonstrated a strong coordination, probably dependent on genetics, between the biophysical structure of wood and physiological plant functions. Thus, the commercial forestry sector could

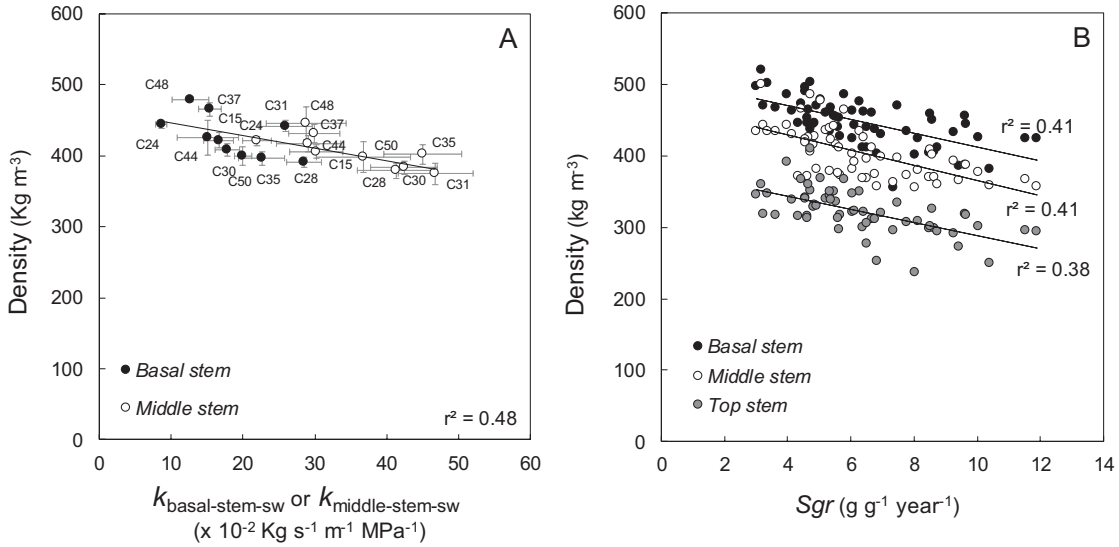

Fig. 7. Relationships between stem hydraulics, wood density, and stem growth rate. (A) Relationship between sapwood-specific hydraulic conductivity of the basal part of the stem ($k_{basal\text{-}stem\text{-}sw}$) and wood density of the basal part of the stem (D_{bYear1}) (black circles), and between sapwood-specific hydraulic conductivity of the middle part of the stem ($k_{middle\text{-}stem\text{-}sw}$) and wood density of the middle part of the stem (D_{mYear1}) (white circles). Each point represents the mean (±SE, n=6) value of these parameters for each different *Pinus radiata* genotype used in the experiment (C15, C24, C28, C30, C31, C35, C37, C44, C48, and C50). (B) Relationship between stem growth rate (Sgr) and wood density of the basal part of the stem (D_{bYear2}) (black circles), wood density of the middle part of the stem (D_{mYear2}) (white circles), and wood density of the top part of the stem (D_{tYear2}) (grey circles). Each point represents an individual plant of the experiment.

identify and select *P. radiata* genotypes with traits that will optimize productivity under specific site conditions, especially water-limited environments under current and future climates.

Supplementary data

The following supplementary data are available at *JXB* online.

Table S1. List of trait abbreviations used in the text.

Table S2. Pearson correlation matrix for the variables belonging to hydraulic traits (HT), normalized hydraulic traits (NHT), gas exchange (GE), wood density (WD), and plant growth rate (PG) based on measurements obtained from 36 trees.

Fig. S1. Factor coordinates of variables on the two first axes of the PCAs for the variables belonging to (A) hydraulic traits (HT), (B) normalized hydraulic traits (NHT), (C) gas exchange (GE), (D) wood density (WD), and (E) plant growth rate (PG).

Acknowledgements

We acknowledge Forest Genetics Ltd. for providing the plant material, and Alan Leckie, Minhuang Wang, and Marta Gallart at Scion. This work was funded by a Scion's post-doctoral fellowship (CO 053 S070 42), Instituto Nacional de Investigación y Tecnología Agraria y Alimentaria (INIA) (DR2015-0402), a National Science Foundation grant (NFS-IOS-1754893), and the French Agence Nationale de la recherche grants (ANR-17-ASIE-0007-02 and ANR-18-PRIM-0006-09).

Author contributions

JRG, JX, MC, PWC, and JCD planned and designed the experiments. JRG performed the experiment and conducted fieldwork. JRG, DFM, and JX analysed the data. JRG, JX, DFM, MC, PWC, and JCD wrote the manuscript.

Data availability

The data supporting the findings of this study are available from the corresponding author, Juan Rodríguez-Gamir, upon request.

References

Aasamaa K, Sõber A. 2001. Hydraulic conductance and stomatal sensitivity to changes of leaf water status in six deciduous tree species. Biologia Plantarum **44**, 65–73.

Albert CH, Thuiller W, Yoccoz NG, Douzet R, Aubert S, Lavorel S. 2010. A multi-trait approach reveals the structure and the relative importance of intra- vs. interspecific variability in plant traits. Functional Ecology **24**, 1192–1201.

Alder NN, Sperry JS, Pockman WT. 1996. Root and stem xylem embolism, stomatal conductance, and leaf turgor in *Acer grandidentatum* populations along a soil moisture gradient. Oecologia **105**, 293–301.

Attia Z, Domec JC, Oren R, Way DA, Moshelion M. 2015. Growth and physiological responses of isohydric and anisohydric poplars to drought. Journal of Experimental Botany **66**, 4373–4381.

Baltunis BS, Brawner JT. 2010. Clonal stability in *Pinus radiata* across New Zealand and Australia. I. Growth and form traits. New Forests **40**, 305–322.

Barotto AJ, Monteoliva S, Gyenge J, Martinez-Meier A, Fernandez ME. 2018. Functional relationships between wood structure and vulnerability to xylem cavitation in races of *Eucalyptus globulus* differing in wood density. Tree Physiology **38**, 243–251.

Black MZ, Patterson KJ, Minchin PE, Gould KS, Clearwater MJ. 2011. Hydraulic responses of whole vines and individual roots of kiwifruit (*Actinidia chinensis*) following root severance. Tree Physiology **31**, 508–518.

Bogeat-Triboulot MB, Martin R, Chatelet D, Cochard H. 2002. Hydraulic conductance of root and shoot measured with the transient and dynamic modes of the high-pressure flowmeter. Annals of Forest Science **59**, 389–396.

Bouffier L, Raffin A, Rozenberg P, Meredieu C, Kremer A. 2009. What are the consequences of growth selection on wood density in the French maritime pine breeding programme? Tree Genetics & Genomes **5**, 11–25.

Bown HE, Watt MS, Mason EG, Clinton PW, Whitehead D. 2009. The influence of nitrogen and phosphorus supply and genotype on mesophyll conductance limitations to photosynthesis in *Pinus radiata*. Tree Physiology **29**, 1143–1151.

Brodribb T, Feild T. 2000. Stem hydraulic supply is linked to leaf photosynthetic capacity: evidence from New Caledonian and Tasmanian rainforests. Plant, Cell & Environment **23**, 1381–1388.

Brodribb T, Holbrook NM, Gutierrez M. 2002. Hydraulic and photosynthetic co-ordination in seasonally dry tropical forest trees. Plant, Cell & Environment **25**, 1435–1444.

Brodribb TJ, Holbrook NM, Zwieniecki MA, Palma B. 2005. Leaf hydraulic capacity in ferns, conifers and angiosperms: impacts on photosynthetic maxima. New Phytologist **165**, 839–846.

Bucci SJ, Goldstein G, Meinzer FC, Franco AC, Campanello P, Scholz FG. 2005. Mechanisms contributing to seasonal homeostasis of minimum leaf water potential and predawn disequilibrium between soil and plant water potential in Neotropical savanna trees. Trees **19**, 296–304.

Bucci SJ, Goldstein G, Meinzer FC, Scholz FG, Franco AC, Bustamante M. 2004. Functional convergence in hydraulic architecture and water relations of tropical savanna trees: from leaf to whole plant. Tree Physiology **24**, 891–899.

Burdon RD, Carson MJ, Shelbourne CJA. 2008. Achievements in forest tree genetic improvement in Australia and New Zealand 10: *Pinus radiata* in New Zealand. Australian Forestry **71**, 263–279.

Carnicer J, Barbeta A, Sperlich D, Coll M, Peñuelas J. 2013. Contrasting trait syndromes in angiosperms and conifers are associated with different responses of tree growth to temperature on a large scale. Frontiers in Plant Science **4**, 409.

Cato S, McMillan L, Donaldson L, Richardson T, Echt C, Gardner R. 2006. Wood formation from the base to the crown in *Pinus radiata*: gradients of tracheid wall thickness, wood density, radial growth rate and gene expression. Plant Molecular Biology **60**, 565–581.

Cernusak LA, Arthur DJ, Pate JS, Farquhar GD. 2003. Water relations link carbon and oxygen isotope discrimination to phloem sap sugar concentration in *Eucalyptus globulus*. Plant Physiology **131**, 1544–1554.

Chave J, Coomes D, Jansen S, Lewis SL, Swenson NG, Zanne AE. 2009. Towards a worldwide wood economics spectrum. Ecology Letters **12**, 351–366.

Chave J, Muller-Landau HC, Baker TR, Easdale TA, ter Steege H, Webb CO. 2006. Regional and phylogenetic variation of wood density across 2456 Neotropical tree species. Ecological Applications **16**, 2356–2367.

Clearwater MJ, Meinzer FC. 2001. Relationships between hydraulic architecture and leaf photosynthetic capacity in nitrogen-fertilized *Eucalyptus grandis* trees. Tree Physiology **21**, 683–690.

Cochard H, Coll L, Le Roux X, Améglio T. 2002. Unraveling the effects of plant hydraulics on stomatal closure during water stress in walnut. Plant Physiology **128**, 282–290.

Conroy J, Milham P, Mazur M, Barlow EWR. 1990. Growth, dry weight partitioning and wood properties of *Pinus radiata* D. Don after two years of CO_2 enrichment. Plant, Cell & Environment **13**, 329–337.

Coruzzi G, Bush DR. 2001. Nitrogen and carbon nutrient and metabolite signaling in plants. Plant Physiology **125**, 61–64.

Cown DJ, Ball RD, Riddell MJC. 2004. Wood density and microfibril angle in 10 *Pinus radiata* clones: distribution and influence on product performance. New Zealand Journal of Forestry Science **34**, 293.

Creese C, Benscoter AM, Maherali H. 2011. Xylem function and climate adaptation in *Pinus*. American Journal of Botany **98**, 1437–1445.

Dalla-Salda G, Martinez-Meier A, Cochard H, Rozenberg P. 2011. Genetic variation of xylem hydraulic properties shows that wood density is involved in adaptation to drought in Douglas-fir (*Pseudotsuga menziesii* (Mirb.)). Annals of Forest Science **68**, 747–757.

Domec JC, Gartner B. 2003. Relationship between growth rates and xylem hydraulic characteristics in young, mature and old-growth ponderosa pine trees. Plant, Cell & Environment **26**, 471–483.

Domec JC, King JS, Ward E, *et al*. 2015. Conversion of natural forests to managed forest plantations decreases tree resistance to prolonged droughts. Forest Ecology and Management **355**, 58–71.

Domec JC, Noormets A, King JS, Sun G, McNulty SG, Gavazzi MJ, Boggs JL, Treasure EA. 2009. Decoupling the influence of leaf and root hydraulic conductances on stomatal conductance and its sensitivity to vapour pressure deficit as soil dries in a drained loblolly pine plantation. Plant, Cell & Environment **32**, 980–991.

Domec JC, Palmroth S, Oren R. 2016. Effects of *Pinus taeda* leaf anatomy on vascular and extravascular leaf hydraulic conductance as influenced by N-fertilization and elevated CO_2. Journal of Plant Hydraulics **3**, E007.

Downes GM, Drew D, Battaglia M, Schulze D. 2009. Measuring and modelling stem growth and wood formation: an overview. Dendrochronologia **27**, 147–157.

Downes GM, Nyakuengama JG, Evans R, Northway R, Blakemore P, Dickson RL, Lausberg M. 2002. Relationship between wood density, microfibril angle and stiffness in thinned and fertilized *Pinus radiata*. IAWA Journal **23**, 253–265.

Drake PL, Price CA, Poot P, Veneklaas EJ. 2015. Isometric partitioning of hydraulic conductance between leaves and stems: balancing safety and efficiency in different growth forms and habitats. Plant, Cell & Environment **38**, 1628–1636.

Dungey H, Brawner J, Burger F, Carson M, Henson M, Jefferson P, Matheson A. 2009. A new breeding strategy for *Pinus radiata* in New Zealand and New South Wales. Silvae Genetica **58**, 28–38.

Euring D, Bai H, Janz D, Polle A. 2014. Nitrogen-driven stem elongation in poplar is linked with wood modification and gene clusters for stress, photosynthesis and cell wall formation. BMC Plant Biology **14**, 391.

Evans GC. 1972. The quantitative analysis of plant growth. Oxford: Blackwell Scientific Publications.

Fan Z-X, Zhang S-B, Hao G-Y, Slik JWF, Cao K-F. 2012. Hydraulic conductivity traits predict growth rates and adult stature of 40 Asian tropical tree species better than wood density. Journal of Ecology **100**, 732–741.

Fichot R, Chamaillard S, Depardieu C, Le Thiec D, Cochard H, Barigah TS, Brignolas F. 2011. Hydraulic efficiency and coordination with xylem resistance to cavitation, leaf function, and growth performance among eight unrelated *Populus deltoides*×*Populus nigra* hybrids. Journal of Experimental Botany **62**, 2093–2106.

Ford ED, Robards AW, Piney MD. 1978. Influence of environmental factors on the production and differentiation in the early wood cells of *Picea sitchensi*s. Annals of Botany **42**, 683–692.

Gallart M, Love J, Meason DF, Coker G, Clinton PW, Xue J, Jameson PE, Klápště J, Turnbull MH. 2019. Field-scale variability in site conditions explain phenotypic plasticity in response to nitrogen source in *Pinus radiata* D. Don. Plant and Soil **443**, 353–368.

Gifford RM, Evans L. 1981. Photosynthesis, carbon partitioning, and yield. Annual Review of Plant Physiology **32**, 485–509.

Hacke UG, Sperry JS, Pittermann J. 2000. Drought experience and cavitation resistance in six shrubs from the Great Basin, Utah. Basic and Applied Ecology **1**, 31–41.

Hacke UG, Sperry JS, Pockman WT, Davis SD, McCulloh KA. 2001. Trends in wood density and structure are linked to prevention of xylem implosion by negative pressure. Oecologia **126**, 457–461.

Hacke UG, Spicer R, Schreiber SG, Plavcová L. 2017. An ecophysiological and developmental perspective on variation in vessel diameter. Plant, Cell & Environment **40**, 831–845.

Hölttä T, Mencuccini M, Nikinmaa E. 2009. Linking phloem function to structure: analysis with a coupled xylem–phloem transport model. Journal of Theoretical Biology **259**, 325–337.

Hubbard R, Ryan M, Stiller V, Sperry J. 2001. Stomatal conductance and photosynthesis vary linearly with plant hydraulic conductance in ponderosa pine. Plant, Cell & Environment **24**, 113–121.

IUCN. 2019. The IUCN red list of threatened species. Version 2018-2. http://www.iucnredlist.org.

Jaquish LL, Ewers FW. 2001. Seasonal conductivity and embolism in the roots and stems of two clonal ring-porous trees, *Sassafras albidum* (Lauraceae) and *Rhus typhina* (Anacardiaceae). American Journal of Botany **88**, 206–212.

Johnson DM, Wortemann R, McCulloh KA, Jordan-Meille L, Ward E, Warren JM, Palmroth S, Domec JC. 2016. A test of the hydraulic vulnerability segmentation hypothesis in angiosperm and conifer tree species. Tree Physiology **36**, 983–993.

Jolliffe IT. 1986. Principal component analysis. New York: Springer Verlag.

Katul G, Leuning R, Oren R. 2003. Relationship between plant hydraulic and biochemical properties derived from a steady-state coupled water and carbon transport model. Plant, Cell & Environment **26**, 339–350.

Kimberley MO, Moore JR, Dungey HS. 2015. Quantification of realised genetic gain in radiata pine and its incorporation into growth and yield modelling systems. Canadian Journal of Forest Research **45**, 1676–1687.

King D, Davies S, Supardi MN, Tan S. 2005. Tree growth is related to light interception and wood density in two mixed dipterocarp forests of Malaysia. Functional Ecology **19**, 445–453.

Knauf M, Köhl M, Mues V, Olschofsky K, Frühwald A. 2015. Modeling the CO_2-effects of forest management and wood usage on a regional basis. Carbon Balance and Management **10**, 13.

Kursar TA, Engelbrecht BMJ, Burke A, Tyree MT, El Omari B, Giraldo JP. 2009. Tolerance to low leaf water status of tropical tree seedlings is related to drought performance and distribution. Functional Ecology **23**, 93–102.

Lachenbruch B, McCulloh KA. 2014. Traits, properties, and performance: how woody plants combine hydraulic and mechanical functions in a cell, tissue, or whole plant. New Phytologist **204**, 747–764.

Laforest-Lapointe I, Martínez-Vilalta J, Retana J. 2014. Intraspecific variability in functional traits matters: case study of Scots pine. Oecologia **175**, 1337–1348.

Lambers H, Chapin FS, Pons TL. 2008. Growth and allocation. In: Plant physiological ecology. New York: Springer, 321–374.

Lasserre JP, Mason EG, Watt MS, Moore JR. 2009. Influence of initial planting spacing and genotype on microfibril angle, wood density, fibre properties and modulus of elasticity in *Pinus radiata* D. Don corewood. Forest Ecology and Management **258**, 1924–1931.

Li X, Wu HX, Southerton SG. 2012. Identification of putative candidate genes for juvenile wood density in *Pinus radiata*. Tree Physiology **32**, 1046–1057.

Marthews TR, Malhi Y, Girardin CA, *et al.* 2012. Simulating forest productivity along a neotropical elevational transect: temperature variation and carbon use efficiency. Global Change Biology **18**, 2882–2898.

Martínez-Vilalta J, Cochard H, Mencuccini M, Sterck F, Herrero A, Korhonen J, Llorens P, Nikinmaa E, Nolè A, Poyatos R. 2009. Hydraulic adjustment of Scots pine across Europe. New Phytologist **184**, 353–364.

Martínez-Vilalta J, Prat E, Oliveras I, Piñol J. 2002. Xylem hydraulic properties of roots and stems of nine Mediterranean woody species. Oecologia **133**, 19–29.

McCulloh KA, Domec JC, Johnson DM, Smith DD, Meinzer FC. 2019. A dynamic yet vulnerable pipeline: integration and coordination of hydraulic traits across whole plants. Plant, Cell & Environment **42**, 2789–2807.

McCulloh KA, Johnson DM, Petitmermet J, McNellis B, Meinzer FC, Lachenbruch B. 2015. A comparison of hydraulic architecture in three similarly sized woody species differing in their maximum potential height. Tree Physiology **35**, 723–731.

McCulloh KA, Meinzer FC, Sperry JS, Lachenbruch B, Voelker SL, Woodruff DR, Domec JC. 2011. Comparative hydraulic architecture of tropical tree species representing a range of successional stages and wood density. Oecologia **167**, 27–37.

Mead DJ. 2013. Sustainable management of *Pinus radiata* plantations. Rome, Italy: FAO.

Meason DF, Baillie BS, Höck B, Lad P, Payn T. 2019. Planted forests and water yield in New Zealand's hydrological landscape—current and future challenges. New Zealand Journal of Forestry **63**, 33–39.

Meinzer FC. 2002. Co-ordination of vapour and liquid phase water transport properties in plants. Plant, Cell & Environment **25**, 265–274.

Meinzer FC, Campanello PI, Domec JC, Genoveva Gatti M, Goldstein G, Villalobos-Vega R, Woodruff DR. 2008. Constraints on physiological function associated with branch architecture and wood density in tropical forest trees. Tree Physiology **28**, 1609–1617.

Meinzer F, Grantz D. 1990. Stomatal and hydraulic conductance in growing sugarcane: stomatal adjustment to water transport capacity. Plant, Cell & Environment **13**, 383–388.

Moore J, Clinton P. 2015. Enhancing the productivity of radiata pine forestry within environmental limits. New Zealand Journal of Forestry **60**, 35–41.

Muller-Landau HC. 2004. Interspecific and inter-site variation in wood specific gravity of tropical trees. Biotropica **36**, 20–32.

Nadezhdina N, Steppe K, De Pauw DJ, Bequet R, Cermak J, Ceulemans R. 2009. Stem-mediated hydraulic redistribution in large roots on opposing sides of a Douglas-fir tree following localized irrigation. New Phytologist **184**, 932–943.

Nicholls J, Waring H. 1977. The effect of environmental factors on wood characteristics. Silvae Genetica **26**, 107–111.

Nicotra AB, Atkin OK, Bonser SP, *et al.* 2010. Plant phenotypic plasticity in a changing climate. Trends in Plant Science **15**, 684–692.

Nikinmaa E, Hölttä T, Hari P, Kolari P, Mäkelä A, Sevanto S, Vesala T. 2013. Assimilate transport in phloem sets conditions for leaf gas exchange. Plant, Cell & Environment **36**, 655–669.

Niklas KJ. 1992. Plant biomechanics: an engineering approach to plant form and function. University of Chicago Press.

Nolf M, Creek D, Duursma R, Holtum J, Mayr S, Choat B. 2015. Stem and leaf hydraulic properties are finely coordinated in three tropical rain forest tree species. Plant, Cell & Environment **38**, 2652–2661.

Oren R, Sperry J, Katul G, Pataki D, Ewers B, Phillips N, Schäfer K. 1999. Survey and synthesis of intra- and interspecific variation in stomatal sensitivity to vapour pressure deficit. Plant, Cell & Environment **22**, 1515–1526.

Pataki DE, Oren R, Phillips N. 1998. Responses of sap flux and stomatal conductance of *Pinus taeda* L. trees to stepwise reductions in leaf area. Journal of Experimental Botany **49**, 871–878.

Paul MJ, Foyer CH. 2001. Sink regulation of photosynthesis. Journal of Experimental Botany **52**, 1383–1400.

Pfautsch S, Renard J, Tjoelker MG, Salih A. 2015. Phloem as capacitor: radial transfer of water into xylem of tree stems occurs via symplastic transport in ray parenchyma. Plant Physiology **167**, 963–971.

Piñol J, Sala A. 2000. Ecological implications of xylem cavitation for several Pinaceae in the Pacific Northern USA. Functional Ecology **14**, 538–545.

Poorter H, Niklas KJ, Reich PB, Oleksyn J, Poot P, Mommer L. 2012. Biomass allocation to leaves, stems and roots: meta-analyses of interspecific variation and environmental control. New Phytologist **193**, 30–50.

Poorter L, Wright SJ, Paz H, *et al.* 2008. Are functional traits good predictors of demographic rates? Evidence from five neotropical forests. Ecology **89**, 1908–1920.

Pratt RB, Jacobsen AL, Ewers FW, Davis SD. 2007. Relationships among xylem transport, biomechanics and storage in stems and roots of nine *Rhamnaceae* species of the California chaparral. New Phytologist **174**, 787–798.

Pratt RB, Jacobsen AL, Hernandez J, Ewers FW, North GB, Davis SD. 2012. Allocation tradeoffs among chaparral shrub seedlings with different life history types (Rhamnaceae). American Journal of Botany **99**, 1464–1476.

Pratt RB, Jacobsen AL, Mohla R, Ewers FW, Davis SD. 2008. Linkage between water stress tolerance and life history type in seedlings of nine chaparral species (*Rhamnaceae*). Journal of Ecology **96**, 1252–1265.

Pratt RB, North GB, Jacobsen AL, Ewers FW. Davis SD. 2010. Xylem root and shoot hydraulics is linked to life history type in chaparral seedlings. Functional Ecology **24**, 70–81.

Price CA, Enquist BJ, Savage VM. 2007. A general model for allometric covariation in botanical form and function. Proceedings of the National Academy of Sciences, USA **104**, 13204–13209.

Rathgeber CB, Decoux V, Leban J-M. 2006. Linking intra-tree-ring wood density variations and tracheid anatomical characteristics in Douglas fir (*Pseudotsuga menziesii* (Mirb.) Franco). Annals of Forest Science **63**, 699–706.

Rodríguez-Gamir J, Primo-Millo E, Forner-Giner MÁ. 2016. An integrated view of whole-tree hydraulic architecture. does stomatal or hydraulic conductance determine whole tree transpiration? PLoS One **11**, e0155246.

Rodríguez-Gamir J, Xue J, Clearwater MJ, Meason DF, Clinton PW, Domec JC. 2019. Aquaporin regulation in roots controls plant hydraulic conductance, stomatal conductance, and leaf water potential in *Pinus radiata* under water stress. Plant, Cell & Environment **42**, 717–729.

Rosner S. 2013. Hydraulic and biomechanical optimization in Norway spruce trunkwood—a review. IAWA Journal **34**, 365–390.

Rosner S, Johnson D, Voggeneder K, Domec JC. 2019. The conifer curve: fast prediction of hydraulic conductivity loss and vulnerability to cavitation. Annals of Forest Science **76**, 82

Sack L, Cowan P, Jaikumar N, Holbrook N. 2003. The 'hydrology'of leaves: co-ordination of structure and function in temperate woody species. Plant, Cell & Environment **26**, 1343–1356.

Sala A, Woodruff DR, Meinzer FC. 2012. Carbon dynamics in trees: feast or famine? Tree Physiology **32**, 764–775.

Salleo S, Trifilò P, Esposito S, Nardini A, Lo Gullo MA. 2009. Starch-to-sugar conversion in wood parenchyma of field-growing *Laurus nobilis* plants: a component of the signal pathway for embolism repair? Functional Plant Biology **36**, 815–825.

Santiago LS, Goldstein G, Meinzer FC, Fisher JB, Machado K, Woodruff D, Jones T. 2004. Leaf photosynthetic traits scale with hydraulic conductivity and wood density in Panamanian forest canopy trees. Oecologia **140**, 543–550.

Savage VM, Bentley LP, Enquist BJ, Sperry JS, Smith DD, Reich PB, von Allmen EI. 2010. Hydraulic trade-offs and space filling enable better predictions of vascular structure and function in plants. Proceedings of the National Academy of Sciences, USA **107**, 22722–22727.

Sevanto S, McDowell NG, Dickman LT, Pangle R, Pockman WT. 2014. How do trees die? A test of the hydraulic failure and carbon starvation hypotheses. Plant, Cell & Environment **37**, 153–161.

Sperry JS. 2011. Hydraulics of vascular water transport. In: Wojtaszek P ed. Signalling and communication in plants: mechanical integration of plant cells and plants. Berlin: Springer, 303–327.

Sperry J, Alder N, Eastlack S. 1993. The effect of reduced hydraulic conductance on stomatal conductance and xylem cavitation. Journal of Experimental Botany **44**, 1075–1082.

Sperry JS, Ikeda T. 1997. Xylem cavitation in roots and stems of Douglas-fir and white fir. Tree Physiology **17**, 275–280.

Stone C, Penman T, Turner R. 2012. Managing drought-induced mortality in *Pinus radiata* plantations under climate change conditions: a local approach using digital camera data. Forest Ecology and Management **265**, 94–101.

Stratton L, Goldstein G, Meinzer F. 2000. Stem water storage capacity and efficiency of water transport: their functional significance in a Hawaiian dry forest. Plant, Cell & Environment **23**, 99–106.

Thomas DS, Montagu KD, Conroy JP. 2007. Temperature effects on wood anatomy, wood density, photosynthesis and biomass partitioning of *Eucalyptus grandis* seedlings. Tree Physiology **27**, 251–260.

Tsuda M, Tyree MT. 2000. Plant hydraulic conductance measured by the high pressure flow meter in crop plants. Journal of Experimental Botany **51**, 823–828.

Tyree MT. 2003. Hydraulic limits on tree performance: transpiration, carbon gain and growth of trees. Trees **17**, 95–100.

Tyree MT, Ewers FW. 1991. The hydraulic architecture of trees and other woody plants. New Phytologist **119**, 345–360.

Tyree MT, Patiño S, Bennink J, Alexander J. 1995. Dynamic measurements of roots hydraulic conductance using a high-pressure flowmeter in the laboratory and field. Journal of Experimental Botany **46**, 83–94.

Tyree MT, Snyderman DA, Wilmot TR, Machado JL. 1991. Water relations and hydraulic architecture of a tropical tree (*Schefflera morototoni*): data, models, and a comparison with two temperate species (*Acer saccharum* and *Thuja occidentalis*). Plant Physiology **96**, 1105–1113.

Tyree MT, Velez V, Dalling JW. 1998. Growth dynamics of root and shoot hydraulic conductance in seedlings of five neotropical tree species: scaling to show possible adaptation to differing light regimes. Oecologia **114**, 293–298.

Tyree MT, Zimmermann MH. 2002. Xylem structure and the ascent of sap. New York: Springer.

Van den Honert TH. 1948. Water transport in plants as a catenary process. Discussions of the Faraday Society **3**, 146–153.

Vander Willigen C, Pammenter NW. 1998. Relationship between growth and xylem hydraulic characteristics of clones of *Eucalyptus* spp. at contrasting sites. Tree Physiology **18**, 595–600.

West GB, Brown JH, Enquist BJ. 1999. A general model for the structure and allometry of plant vascular systems. Nature **400**, 664–667.

Wright SJ, Kitajima K, Kraft NJ, *et al.* 2010. Functional traits and the growth–mortality trade-off in tropical trees. Ecology **91**, 3664–3674.

Wu HX, Eldridge KG, Matheson AC, Powell MB, McRae TA, Butcher TB, Johnson IG. 2007. Achievements in forest tree improvement in Australia and New Zealand 8. Successful introduction and breeding of radiata pine in Australia. Australian Forestry **70**, 215–225.

Zhang YJ, Meinzer FC, Hao GY, *et al.* 2009. Size-dependent mortality in a Neotropical savanna tree: the role of height-related adjustments in hydraulic architecture and carbon allocation. Plant, Cell & Environment **32**, 1456–1466.

Zhu SD, Song JJ, Li RH, Ye Q. 2013. Plant hydraulics and photosynthesis of 34 woody species from different successional stages of subtropical forests. Plant, Cell & Environment **36**, 879–891.

Zimmermann MH. 1983. Xylem structure and the ascent of sap. Springer-Verlag.